Volume 60   1 September 2014   ISSN 0043-1354

ELSEVIER

IWA the international water association

WATER RESEARCH

A Journal of the International Water Association

Available online at www.sciencedirect.com

ScienceDirect

journal homepage: www.elsevier.com/locate/watres

ELSEVIER

CrossMark
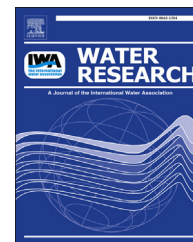
Trading oxidation power for efficiency: Differential inhibition of photo-generated hydroxyl radicals versus singlet oxygen

Jonathon Brame [a], Mingce Long [b], Qilin Li [a], Pedro Alvarez [a,*]

[a] Rice University, Department of Civil and Environmental Engineering, United States
[b] Shanghai Jiao Tong University, School of Environmental Science and Engineering, United States

ARTICLE INFO

ABSTRACT

The ability of reactive oxygen species (ROS) to interact with target pollutants is crucial for efficient water treatment using advanced oxidation processes (AOPs), and inhibition by natural organic matter (NOM) can significantly reduce degradation efficiency. We compare $OH^{\bullet}$-based degradation (H_2O_2-UV) to $^1O_2$-based degradation (Rose Bengal) of several probe compounds (furfuryl alcohol, ranitidine, cimetidine) interacting in water containing background constituents likely to be found in treatment water such as natural organic matter (NOM) and phosphate, as well as in effluent from a waste-water treatment plant (WWTP). Hydroxyl radicals were much more susceptible to hindrance by all three background matrices (NOM, phosphate and WWTP effluent) tested, while $^1O_2$ was only slightly inhibited by NOM and not by phosphate or WWTP effluent. A mechanistic model accounting for this inhibition in terms of radical scavenging and inner filter effects was developed, and accurately simulated the results of the NOM interactions. These results underscore the importance of considering the effect of background constituents in the selection of photocatalysts and in the design of AOPs for emerging applications in tertiary treatment of wastewater effluent and disinfection of natural waters.

© 2014 Elsevier Ltd. All rights reserved.

1. Introduction

As the demand for clean water continues to grow, the necessity for advanced water treatment and reclamation technologies will continue to increase (Brame et al., 2011; Qu et al., 2012). Advanced oxidation processes (AOP) have great potential to remove many common water pollutants as well as contaminants of emerging concern such as pharmaceutical products, endocrine disrupting compounds, and pesticides (Chong et al., 2010; Herrmann, 1999; Klavarioti et al., 2009).

Reactive oxygen species (ROS) such as hydroxyl radical ($OH^{\bullet}$) and singlet oxygen ($^1O_2$) that are generated in photocatalytic and photochemical AOPs can oxidize recalcitrant organic and biological contaminants with much lower potential to form carcinogenic disinfection byproducts common to chemical treatment approaches such as chlorination and ozonation (Li et al., 2008; Qu et al., 2012; Toor and Mohseni, 2007). However, the efficiency of AOPs can be hindered by the presence of background constituents in water, such as organic material (e.g., natural organic matter [NOM] or wastewater treatment plant effluent) or inorganic ions (e.g., phosphate)

(Abdullah et al., 1990; Enriquez and Pichat, 2001; Lee et al., 2011). Such background constituents can interfere with ROS-based degradation processes by absorbing incoming light and by acting as radical scavengers, reducing both the amount of ROS produced and the effective concentration of ROS available for interaction with the target pollutants.

An important factor in whether or not background organic material will significantly affect degradation treatment efficiency is the selectivity of the generated ROS (Hoigné and Bader, 1983; Kim et al., 2012; Lee and von Gunten, 2010). Hydroxyl radicals, which are the primary ROS produced by TiO_2 photocatalysis and H_2O_2/UV oxidation, are very powerful oxidants (2.8 V vs. standard hydrogen electrode (SHE) (Klamerth et al., 2012)), and are therefore able to oxidize a broad range of organic compounds. However hydroxyl radicals are also non-specific, making them susceptible to scavenging by non-target organic and inorganic compounds in water, and their generation requires UV light, which is partially absorbed by organic material in the water (Edzwald et al., 1985; Korshin et al., 1997). Singlet oxygen is produced by visible-light active photosensitizers such as fullerenes (C_{60}), porphyrins and Rose Bengal (RB). Since light absorption by NOM is greatest in the far UV and declines throughout the UV and visible spectrum (Edzwald et al., 1985; Korshin et al., 1997), NOM inner filtering is likely less inhibitory to visible light-activated photocatalysts. Furthermore, $^1O_2$ is much more selective than OH•, targeting electron-rich moieties in pollutants such as phenols and activated aromatics (Lee and von Gunten, 2010). Although this specificity could decrease the probability of inadvertent scavenging by organic matter in natural waters, $^1O_2$ is a much weaker oxidant (1.1 V vs. SHE (Ahmad and Armstrong, 1984)) than OH•, possibly resulting in partial oxidation of some compounds, including formation of potentially harmful oxidation byproducts (e.g., quinones, nitrophenols, aldehydes, etc. (Chen et al., 1998; Dzengel et al., 1998; Echavia et al., 2009; Topudurti et al., 1998)). A weaker oxidant may also require longer contact times or more photosensitizing material for the same degradation capacity, and not allow degradation of some materials that require strong oxidation.

Most ROS-generating photoreactive and photocatalytic degradation studies are conducted using laboratory-grade deionized water, which ignores these inhibitory effects of background constituents in natural water. Recently, more research has been conducted using non-ideal water sources, specifically focusing on wastewater treatment plant (WWTP) effluent, since tertiary treatment is a likely application scenario for AOP technology (Kim et al., 2012; Klamerth et al., 2012). We recently demonstrated that selective ROS can be more efficient than non-selective ROS in removal of some organic contaminants (Kim et al., 2012), and others have done similar work in wastewater effluent (Lee and von Gunten, 2010), but this tradeoff between oxidative power and specificity in photocatalytic AOPs has not been systematically explored in the literature. This is a critical knowledge gap because inhibition of ROS-mediated degradation by naturally occurring organic matter could have a significant impact on the degradation efficiency of this technology upon implementation.

In this paper we consider two representative types of ROS commonly involved in photo-active AOPs ($^1O_2$ and OH•) as produced by homogeneous photoreactive chemicals as part of a larger study to determine the effect and mechanisms of organic matter and inorganic inhibition of ROS-assisted photochemical degradation. Homogeneous photoreactive materials were selected to remove confounding surface effects of heterogeneous photocatalysts (e.g., sorption, charge transfer interference, local vs. bulk ROS scavenging) and focus on the interaction between photo-generated ROS and background organic materials. We explore the extent to which common water constituents such as natural organic matter and phosphate, as well as constituents in WWTP effluent decrease degradation rates and ROS production capacity within the context of water treatment, and develop a mechanistic model to account for the decreased efficiency due to scavenging of ROS and light absorption by NOM (inner filter effect).

2. Materials and methods

2.1. Photo-reactive testing

Hydrogen peroxide (H_2O_2) illuminated by UV light (254 nm) was used to produce hydroxyl radicals (OH•), and Rose Bengal (RB) illuminated by visible light (400—800 nm) was used to produce singlet oxygen ($^1O_2$). H_2O_2 was 35% H_2O_2 supplied by Fischer Scientific. RB was supplied by Sigma—Aldrich. Photosensitizer (H_2O_2, RB) concentrations were 15 and 25 ppm respectively, which were chosen to match the steady state ROS production of traditional photocatalyst materials in DI water (Brame et al., 2013; Liao et al., 2013) as part of a larger study of ROS production.

Illumination occurred within a photoreactor described previously (Brame et al., 2013; Liao et al., 2013), with UV-C bulbs (H_2O_2, 254 nm) or visible bulbs (RB; 400—800 nm). Photo-reactive materials were stirred vigorously in a quartz reaction vessel with 1 mL sample aliquots taken at various time points for analysis. Degradation of a probe compound easily oxidized by both hydroxyl radicals and singlet oxygen (furfuryl alcohol [FFA], Sigma—Aldrich) was used as a surrogate for ROS production (Buxton et al., 1988; Haag and Hoigne, 1986; Lee et al., 2009, 2010; Minero et al., 2000), which was confirmed using electron paramagnetic resonance (EPR) spectrometry (Liao et al., 2013). Ranitidine (N-(2-[(5-[[(dimethylamino)methyl]furan-2-yl)methylthio]ethyl)-N′-methyl-2-nitroethene-1,1-diamine) and cimetidine (2-cyano- 1-methyl-3-(2-[(5-methyl- 1H-imidazol- 4-yl)methylthio]ethyl)guanidine), two pharmaceutical compounds, were also used as representative target pollutants (Sigma—Aldrich). Dark and non-reactive controls were run to ensure that degradation was the result of photoreactive ROS interactions.

2.2. Analysis

Quantification of FFA concentration was carried out with a Shimadzu Prominence HPLC (Shimadzu Corp., Columbia MD) using a C18 column with acetonitrile and 0.1% (w/v) phosphoric acid as mobile phase solvents (70:30). First order degradation rate constants (k_{obs}) were calculated from a linear regression of observed exponential decay. Determination of

the absorption coefficient as a function of wavelength, $\alpha(\lambda)$, for the various compounds used in this study was measured using an Ultraspec 2100 Pro UV/Vis spectrophotometer and a 1 cm (pathlength) quartz cuvette. ROS production and quenching were confirmed by EPR measurement using a Varian E-6 spectrometer under the following conditions: temperature = 293 K; microwave frequency = 9.225 GHz; microwave power = 10 mW; modulation amplitude = 1 G at 100 kHz; and scan time = 4 s. Since ROS are extremely short-lived, the compounds 2,2,6,6-tetramethyl-4-piperidinol (TMP)(Lee et al., 2009; Liao et al., 2013) and α-(4-pyridyl-1-oxide)-N-*tert*-butylnitrone (POBN)(Huling et al., 1998) were used as spin-trapping agents to measure $^1O_2$ and OH$^\bullet$ production, respectively. Upon interaction with radical species, spin traps form spin adducts which are identified by their EPR spectrum. TMP is oxidized when it interacts with singlet oxygen to form 2,2,6,6-tetramethyl-4-piperidinol-N-oxyl radical (TMPN), which can similarly be identified by EPR. The spectra obtained were representative of OH$^\bullet$ and $^1O_2$ radical species (Liao et al., 2013). All solvents were analytical-grade and obtained from Sigma—Aldrich.

2.3. Inhibitory compounds

Three different natural water matrices (natural organic matter, phosphate and wastewater treatment effluent) were used to determine their effect on the degradation efficiency of photo-produced ROS. Suwannee River natural organic matter (SR-NOM) was obtained from the International Humic Substances Society (St. Paul, MN, USA) (Hyung et al., 2006). Phosphate (Na$_3$PO$_4$, Sigma—Aldrich) was mixed into a 1 M stock solution with the pH adjusted to 7.0. This stock solution was then diluted for individual tests. Wastewater effluent (BOD$_5$ = 2.4 mg L^{-1}, TSS = 4.3 mg L^{-1}, NH$_3$ = 0.9 mg L^{-1}, DO = 6.2 mg L^{-1}) was obtained post-treatment from the Houston 69th street wastewater treatment plant and used without modification or dilution. The pH of all samples was circum-neutral (5—7) and no pH adjustments were made.

2.4. ROS production

Steady state ROS generation was measured using FFA as a probe compound. ROS-mediated degradation of simple organics in DI water can be modeled as a second order reaction:

$$\frac{d[A]}{dt} = k_{ROS,A} * [ROS]*[A] \tag{1}$$

Here A represents the compound being degraded (e.g., FFA) and $k_{ROS,A}$ is the reaction rate constant for a specific ROS compound reacting with A. Values of $k_{ROS,A}$ for a variety of target compounds (A) in water are available for both OH$^\bullet$ (Buxton et al., 1988) and $^1O_2$ (Wilkinson et al., 1995). Since ROS species are short-lived compared to experimental time-scales (Tachikawa and Majima, 2009), steady state is often assumed (Wilkinson et al., 1995), simplifying Eq. (1) to a first-order differential equation:

$$[ROS] = [ROS]_{SS} \tag{2}$$

$$\frac{d[A]}{dt} = k_{ROS,A} * [ROS]_{SS}*[A] \tag{3}$$

$$\frac{d[A]}{dt} = k_{obs}*[A] \tag{4}$$

$$k_{obs} = k_{ROS,A} * [ROS]_{SS} \tag{5}$$

By modeling the measured degradation loss of compound A as an exponential decay we can determine the observed degradation rate constant, k_{obs}, as the slope of a log-normal plot of [A] vs. time. Only initial degradation data ($\sim$30% removal) was used to calculate k_{obs} to avoid confounding effects of degradation products. By combining measured k_{obs} values with k_{ROS} values from the literature we can determine the steady state ROS concentration using Eq. (5) (Table 1).

First-order FFA degradation rate constants (k_{obs}) were measured for hydroxyl radical- and singlet oxygen-based photodegradation processes in the presence of SR-NOM. The concentration of NOM was increased up to 25 mg L^{-1} to simulate a range of realistic environmental concentrations (Ma et al., 2001; Thurman, 1985). Since Eq. (1) no longer applies with NOM as an additional reactant with generated ROS, k_{obs} values were measured to determine the effect of NOM on the overall degradation capacity of the different photosensitizing materials. Additionally, we measured the degradation rate of NOM by both OH$^\bullet$ and $^1O_2$ (Table 1) to determine the value of k_{ROS} for NOM degradation by photo-produced ROS. Due to the heterogeneous composition of NOM, UV 254 absorbance was used as a proxy for NOM concentration (Kerc et al., 2003). Although photosensitization of dissolved organic matter irradiated by natural sunlight has been shown to contribute to photodegradation of organic contaminants (Chin et al., 2004), we observed no significant FFA degradation in the absence of photosensitive materials (H$_2$O$_2$, RB) up to 25 mg L^{-1} SR-NOM (SI-Fig. S1).

3. Results and discussion

3.1. Inhibition by background water constituents

3.1.1. NOM
Dissolved NOM (Steinberg et al., 2006) had a more pronounced adverse effect on OH$^\bullet$-mediated degradation compared to $^1O_2$ degradation (Fig. 1). The addition of 25 mg L^{-1} NOM reduced the OH$^\bullet$-mediated FFA degradation rate constant (k_{obs}) by over 60%. Even at lower NOM concentrations the H$_2$O$_2$ photocatalytic FFA degradation rate was significantly reduced. Meanwhile 25 mg L^{-1} NOM reduced the $^1O_2$-mediated FFA degradation rate constant by less than 20%. NOM is a complex mixture of organic materials including a small fraction of electron-rich moieties such as olefinic compounds and aromatic alcohols (Huang et al., 2004; Maximov and Glebko, 1974; Schnitzer and Khan, 1972). Singlet oxygen reacts primarily with this smaller, more hydrophobic fraction of the NOM mixture while OH$^\bullet$ is reactive with a much larger fraction, and we believe this exclusivity makes $^1O_2$-producing processes less susceptible to scavenging by NOM (Maximov and Glebko, 1974; Schnitzer and Vendette, 1975). This greater effect of NOM on OH$^\bullet$ compared to $^1O_2$-based photodegradation

Table 1 – Degradation rate constants for the degradation of furfuryl alcohol in DI water (FFA/DI), and of FFA in the presence of 25 mg/L NOM (FFA/NOM), and of the degradation of natural organic matter (NOM) as measured in this study, as well as the steady state ROS concentrations calculated from FFA degradation rates in DI water and literature values of k_{ROS} (Buxton et al., 1988; Wilkinson et al., 1995).

	OH• Generation (H_2O_2)			$^1O_2$ Generation (RB)		
	FFA/DI	FFA/NOM	NOM	FFA/DI	FFA/NOM	NOM
k_{OBS} (min^{-1}, $\times 10^{-3}$)	49.5 ± 4.5	18.9 ± 1.6	16.8 ± 5.9	3.7 ± 0.1	2.9 ± 0.2	0.1 ± 0.01
$[ROS]_{SS}$ (M, $\times 10^{-15}$)	55.0 ± 4.9			564.0 ± 60.4		

processes shows the impact of background organic material in the degradation process (Enriquez and Pichat, 2001; Minero et al., 1999; Schmelling et al., 1997).

3.1.2. Phosphate

Background concentrations of phosphate (60–3000 mg L^{-1} PO_4^{3-}) also had a greater inhibitory effect on photocatalytic degradation of FFA by OH• compared to $^1O_2$, with the OH•-mediated degradation rate constant being reduced by more than 50% and the $^1O_2$-mediated degradation unaffected (Fig. 2). A comparable overall decrease in the photocatalytic degradation efficiency of several organic compounds in the presence of a similar phosphate concentration range has been reported with TiO$_2$ photocatalysis (Abdullah et al., 1990), although the degradation efficiency fell off much more quickly (more inhibition at lower concentration, similar inhibition at higher concentration). This effect is commonly attributed to competitive adsorption effects (Guillard et al., 2005; Pereira et al., 2013), or to trapping of OH• at the photocatalyst surface (Guillard et al., 2005; Kormann et al., 1991). However, neither of these effects is possible in our homogeneous system. Additionally, because the phosphate buffer was neutral (pH 7.0), the pH of the system remained unchanged, and pH-dependent effects were unlikely. Therefore, we attribute the

decrease in FFA degradation to radical scavenging by phosphate. The reaction rate constant for OH• interaction with phosphate is significantly lower than for interaction with FFA (Buxton et al., 1988), however, as the phosphate concentration increases so does its contribution to scavenging (Fig. 2). At 3000 mg/L (the highest phosphate concentration tested), the degradation rate of FFA and phosphate should be similar (calculated from Eq. (1), where the term $k_{ROS,A}$*[A] is similar for phosphate and for FFA), indicating that scavenging could play a significant role in degradation inhibition. This is further validated by the lack of inhibition of FFA degradation by $^1O_2$ in the RB system, which is expected since the redox potential of phosphate (2.65 V vs. standard hydrogen electrode (Brusa and Grela, 2003)) allows oxidation by OH• (2.8 V) but not by $^1O_2$ (1.1 V). In heterogeneous systems this effect is often ignored in favor of surface interactions (Abdullah et al., 1990; Guillard et al., 2005); however, this test shows that scavenging of produced radicals by background inorganic ions can significantly reduce the degradation efficiency of OH• generating systems.

3.1.3. Wastewater effluent

Since tertiary treatment at wastewater treatment facilities is a likely implementation scenario for ROS-based treatment
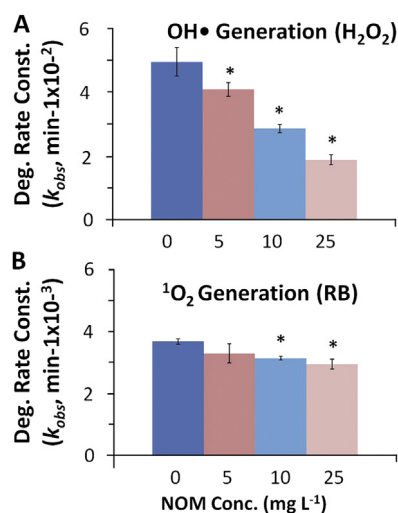
Fig. 1 – First-order FFA degradation rate constants (k_{obs}) of OH• generated by H_2O_2 (A) and $^1O_2$ generated by RB (B) in deionized water (DI) with increasing concentrations of Suwanee River natural organic matter (NOM). [FFA]$_0$ = 25 mg L^{-1}, [H_2O_2] = 15 mg L^{-1}, [RB] = 25 mg L^{-1}. Error bars represent one standard deviation from the mean of triplicate measurements, (*) represents statistically significant difference between sample and distilled water (DI) control.
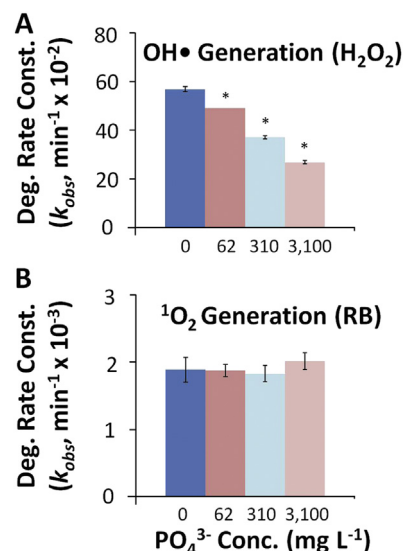
Fig. 2 – First-order FFA degradation rate constants (k_{obs}) of OH• generated by H_2O_2 (A) and $^1O_2$ generated by RB (B) in deionized water (DI) with increasing concentrations of phosphate. [FFA]$_0$ = 25 mg L^{-1}, [H_2O_2] = 15 mg L^{-1}, [RB] = 25 mg L^{-1}. Error bars represent one standard deviation from the mean of triplicate measurements, (*) represents statistically significant difference between sample and distilled water (DI) control.

systems, we also examined the inhibitory effect of organic matter in the effluent of a wastewater treatment plant on photo-generated OH• and $^1O_2$. The rate of FFA degradation by OH• from H_2O_2 was reduced by 30% (Fig. 3A). In contrast, the singlet oxygen-mediated FFA degradation rate was not significantly reduced (Fig. 3B). Apparently, even water that has been pre-treated in a wastewater treatment plant contains enough background material to significantly reduce degradation efficiency, and the extent of this inhibitory effect will vary based on the treatment conditions and type of ROS being used.

3.2. Degradation of pharmaceuticals

The presence of 25 mg L^{-1} NOM significantly decreased the OH•-mediated degradation rate for both ranitidine and cimetidine (Fig. 4A). The OH• treatments experienced a 75–80% decrease in first-order degradation rate constants, whereas $^1O_2$-based degradation rates were mostly unaffected. The removal of pharmaceutical compounds (such as cimetidine and ranitidine), personal care products and other pollutants of emerging concern from wastewater is an important issue in water treatment due to unintended effects on downstream receptors (Fent et al., 2006; Kim et al., 2007; Snyder et al., 2005). The possibility of beneficial reuse and eventual recycling of wastewater into potable water requires efficient removal of these compounds, many of which are resistant to contemporary wastewater treatment strategies (Brame et al., 2011; Qu et al., 2012; Ternes et al., 2003). The differential inhibition between OH•- and $^1O_2$-mediated removal of these model pharmaceuticals (Fig. 4) corroborates the high likelihood of inhibition due to background materials in AOP systems as demonstrated in Section 3.1. These compounds are representative of those likely to be targeted in advanced oxidation treatments, again verifying the need to determine the extent of oxidative inhibition from background materials prior to implementation of these technologies.
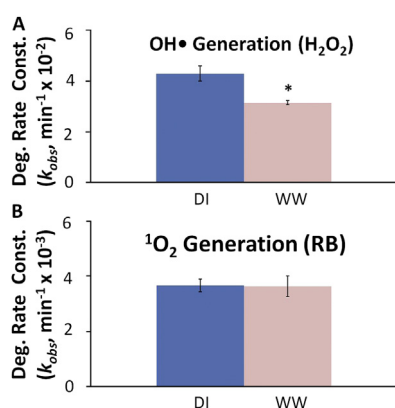
Fig. 3 – First-order FFA degradation rate constants (k_{obs}) of OH• generated by H_2O_2 (A) and $^1O_2$ generated by RB (B) in purified deionized water (DI) and effluent from the Houston 69th Street wastewater treatment plant (WW).
[FFA]$_0$ = 25 mg L^{-1}, [H_2O_2] = 15 mg L^{-1}, [RB] = 25 mg L^{-1}. Error bars represent one standard deviation from the mean of triplicate measurements, (*) represents statistically significant difference between DI and WW treatments ($p < 0.05$).
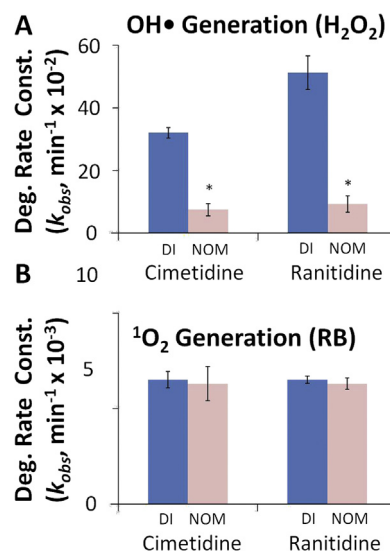
Fig. 4 – First order degradation rate constants for OH•-mediated degradation (A) and $^1O_2$–mediated degradation (B) of ranitidine and cimetidine in DI water and with 25 mg L^{-1} NOM. [ranitidine]$_0$ = [cimetidine]$_0$ = 25 mg L^{-1}, [H_2O_2] = 15 mg L^{-1}, [RB] = 25 mg L^{-1}. Error bars represent one standard deviation from the mean of triplicate measurements, (*) represents statistically significant difference between DI and NOM treatments ($p < 0.05$).

3.3. Inhibition mechanisms

With no confounding surface effects due to our choice of homogeneous reactants, degradation inhibition is limited to scavenging of produced ROS by non-target organic species, and decreasing ROS production due to background materials blocking or absorbing light (inner filter effect)(Guillard et al., 2005).

3.3.1. Scavenging by non-target compounds
The degradation of potential scavenging compounds (such as NOM) in water can be described similar to Eq. (1):

$$\frac{d[Sc]}{dt} = k_{ROS,Sc} * [ROS]*[NOM] \tag{6}$$

Assuming that ROS loss is due to reactions with either the target compound (A) or the scavenging compound (NOM), a mass balance on the ROS in the system yields:

$$\frac{d[ROS]}{dt} = P_{ROS} - k_{ROS,A} * [ROS] * [A] - k_{ROS,NOM} * [ROS] * [NOM] \tag{7}$$

where P_{ROS} represents the production rate of ROS. At steady state, P_{ROS} is equal to the sum of the degradation terms, and the equation can be solved for $[ROS]_{ss}$:

$$[ROS]_{ss} = \frac{P_{ROS}}{k_{ROS,A} * [A] + k_{ROS,NOM} * [NOM]} \tag{8}$$

Inserting Eq. (8) into Eq. (3) provides an expression for the degradation rate of compound A in the presence of a scavenging compound (NOM):

$$\frac{d[A]}{dt} = \frac{k_{ROS,A} * [A] * P_{ROS}}{k_{ROS,A} * [A] + k_{ROS,NOM} * [NOM]} = \frac{P_{ROS}}{1 + \frac{k_{ROS,NOM} * [NOM]}{k_{ROS,A} * [A]}} \quad (9)$$

The value of $k_{ROS,A}$ for FFA degradation by OH• and $^1O_2$ are available in the literature (Buxton et al., 1988; Wilkinson et al., 1995), while $k_{ROS,NOM}$ was determined by measuring the degradation of NOM (via decrease in UV 254 absorbance) by ROS in the absence of FFA. P_{ROS} is equal to the steady state degradation rate of compound A in the absence of NOM (Eq. (1) inserted into Eq. (7) with [Sc] = 0).

3.3.2. Inner filter effect

Natural organic matter absorbs light in both the visible and UV spectrums, diminishing the illumination intensity available for ROS production (Schindelin and Frimmel, 2000; Sorensen et al., 1996) and decreasing P_{ROS}. This inner filter effect (Kubista et al., 1994) can be accounted for by measuring the absorbance (Abs) of a concentration of NOM, which is proportional to the effective path length of the light (ℓ_{eff}) (Bezares-Cruz et al., 2004):

$$Abs = \alpha * \ell_{eff} * [NOM] \quad (10)$$

$$\frac{I}{I_0} = 10^{-\alpha * \ell_{eff} * [NOM]} \quad (11)$$

The absorption coefficient (α) can be determined spectroscopically as a function of wavelength for a given NOM concentration, [NOM]. The overall decrease in ROS production is proportional to the decrease in transmitted illumination intensity over the entire reaction volume, which can be calculated as a function of both wavelength (λ) and path length (ℓ_{eff}) for a given reactor geometry. For our cylindrical reactor, the decrease in transmitted light can be expressed in integral form as:

$$\int_{\lambda_1}^{\lambda_2} \int_0^V \frac{I(\ell,\lambda) * dV * d\lambda}{V} = \int_{\lambda_1}^{\lambda_2} \int_0^R \frac{I(\ell,\lambda) * 2\pi\ell h * d\ell * d\lambda}{\pi R^2 h}$$

$$= \frac{2}{R^2} \int_{\lambda_1}^{\lambda_2} \int_0^R 10^{-\alpha(\lambda) * [NOM] * (R-\ell)} * \ell * dl * d\lambda \quad (12)$$

This expression can then be numerically integrated using the spectroscopic data for $\alpha(\lambda)$ to obtain the decrease in illumination intensity and therefore the decrease in ROS production for a given NOM concentration. This decrease in transmitted illumination intensity is proportional to the decrease in P_{ROS} in the system. Inserting this value into Eq. (9) allows us to model the decrease in degradation rate (relative to uninhibited degradation) as a function of NOM concentration.

Fig. 5 shows the relative inhibition of the scavenging model and the inner filter model individually, as well as the total effect of these two inhibition mechanism (Eq. (12) inserted as P_{ROS} into Eq. (9)) compared to the measured degradation data. The combination of these two effects matches the data quite well, with $r^2 > 0.99$. In the case of OH• generation both scavenging and light filtering play a significant role, although scavenging is much more inhibitory than filtering of light by NOM in solution. For $^1O_2$, however, scavenging is negligible and any loss of efficiency is due to the inner filter effect.
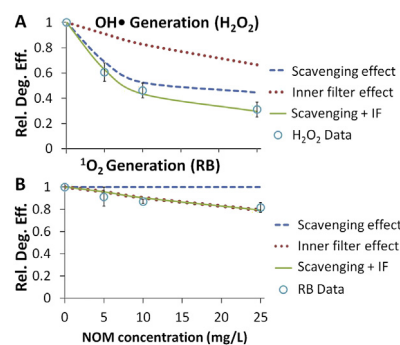
Fig. 5 – Modeled contribution of ROS scavenging (··) and inner filtering (IF; ---) of light on the degradation efficiency relative to clean water as a function of NOM concentration for OH• production (A) and $^1O_2$ production (B). The combination of these two effects (–) matches very well with the measured data (○), with $r^2 > 0.99$.

3.4. EPR confirmation of ROS

EPR measurements confirmed the presence of OH• and $^1O_2$ ROS and showed a significant decrease in OH• with the addition of 25 mg L^{-1} NOM (Fig. 6). The amplitude of the EPR spectrum is qualitatively proportional to the ROS concentration for a given species (Paul et al., 2006), thus the addition of NOM clearly reduces the available OH•. Since the EPR reaction takes place in a small capillary tube, the reaction volume and light path length are both significantly smaller than in our batch ROS tests. Because of the shorter path length the inner filter effect is negligible in EPR tests, so the only mechanism for reduction in ROS concentration is radical scavenging. Interestingly, there is no apparent decrease in the $^1O_2$ spectra with NOM, even though FFA degradation decreased by almost 20% with 25 mg L^{-1} NOM. This confirms that the decrease in $^1O_2$ degradation efficiency is likely due more to light filtering than scavenging effects. These results confirm the ROS
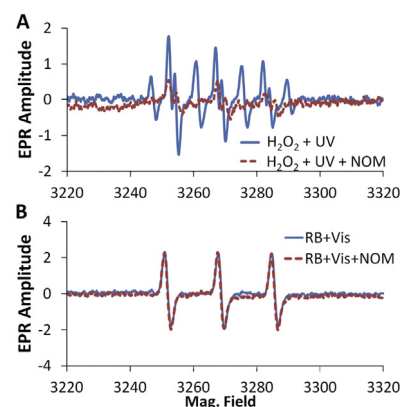
Fig. 6 – EPR spectra showing (A) OH• production (with spin trapping agent POBN) by H$_2O_2$, and (B) $^1O_2$ production (per TMP oxidation) by RB. EPR amplitude is proportional to the quantity of ROS produced. (A) clearly shows a significantly decreased amplitude with the addition of NOM, while the EPR amplitudes of (B) remains unchanged.
[H$_2O_2$] = 15 mg L^{-1}, [RB] = 25 mg L^{-1}, [NOM] = 25 mg L^{-1}.

production by the various photosensitizing materials and show confirmatory evidence that NOM scavenges OH• more preferentially than $^1O_2$.

4. Conclusions

Although hydroxyl radicals are more powerful oxidants than singlet oxygen, which may make them more effective for some applications, they are much more prone to efficiency loss in complex water matrices. Because singlet oxygen is a more selective oxidant, preferentially oxidizing more electron-rich compounds, it is less likely to be affected by aqueous organic matter in natural waters. Further study is needed to determine if other selective oxidants (i.e., ozone, sulfate radicals, chlorine, etc. (Lee and von Gunten, 2010)) deliver efficiency advantages in the presence of background materials similar to $^1O_2$. Additionally, the inner filter effect of NOM can be a significant concern when treatment volumes and illumination path lengths are large. Due to these unique strengths and weaknesses there may be some applications that are better suited for OH• advanced oxidation treatment (e.g., systems with relatively clean water or contaminants requiring especially strong oxidation), and some that are better suited for singlet oxygen advanced oxidation treatment (e.g., when organic matter, phosphate and other background constituents could cause inhibition and significantly reduce the treatment efficiency). There may also be treatment scenarios in which a combination of ROS species (concurrent or sequential) would allow a high level of treatment by combining the oxidation strength of hydroxyl radicals and the selectivity of singlet oxygen. In addition to considerations of the efficiency of different ROS types, it is essential that care be taken to avoid the formation of byproducts which can potentially be more harmful than the original contaminant, especially when using a weaker oxidant for which achieving complete mineralization may be more difficult. Overall, this work underscores the importance of careful evaluation of the system-specific ROS inhibition potential for the selection of photocatalysts and design of resilient AOPs.

Acknowledgments

Appendix A. Supplementary data

Supplementary data related to this article can be found at http://dx.doi.org/10.1016/j.watres.2014.05.005.

REFERENCES

Abdullah, M., Low, G.K.C., Matthews, R.W., 1990. Effects of common inorganic anions on rates of photocatalytic oxidation of organic carbon over illuminated titanium dioxide. J. Phys. Chem. 94 (17), 6820—6825.

Ahmad, R., Armstrong, D.A., 1984. The effect of pH and complexation on redox reactions between RS• radicals and flavins. Can. J. Chem. 62 (1), 171—177.

Bezares-Cruz, J., Jafvert, C.T., Hua, I., 2004. Solar photodecomposition of decabromodiphenyl ether: products and quantum yield. Environ. Sci. Technol. 38 (15), 4149—4156.

Brame, J., Li, Q.L., Alvarez, P.J.J., 2011. Nanotechnology-enabled water treatment and reuse: emerging opportunities and challenges for developing countries. Trends Food Sci. Technol. 22 (11), 618—624.

Brame, J.A., Hong, S.W., Lee, J., Lee, S.-H., Alvarez, P.J.J., 2013. Photocatalytic pre-treatment with food-grade TiO2 increases the bioavailability and bioremediation potential of weathered oil from the deepwater horizon oil spill in the Gulf of Mexico. Chemosphere 90 (8), 2315—2319.

Brusa, M.A., Grela, M.A., 2003. Experimental upper bound on phosphate radical production in TiO2 photocatalytic transformations in the presence of phosphate ions. Phys. Chem. Chem. Phys. 5 (15), 3294—3298.

Buxton, G.V., Greenstock, C.L., Helman, W.P., Ross, A.B., 1988. Critical review of rate constants for reactions of hydrated electrons, hydrogen atoms and hydroxyl radicals (.OH/.O-) in aqueous solution. J. Phys. Chem. Ref. Data 17 (2), 513—886.

Chen, W., Koenigs, L.L., Thompson, S.J., Peter, R.M., Rettie, A.E., Trager, W.F., Nelson, S.D., 1998. Oxidation of acetaminophen to its toxic quinone imine and nontoxic catechol metabolites by baculovirus-expressed and purified human cytochromes P450 2E1 and 2A6. Chem. Res. Toxicol. 11 (4), 295—301.

Chin, Y.-P., Miller, P.L., Zeng, L., Cawley, K., Weavers, L.K., 2004. Photosensitized degradation of bisphenol a by dissolved organic matter. Environ. Sci. Technol. 38 (22), 5888—5894.

Chong, M.N., Jin, B., Chow, C.W.K., Saint, C., 2010. Recent developments in photocatalytic water treatment technology: a review. Water Res. 44 (10), 2997—3027.

Dzengel, J., Theurich, J., Bahnemann, D.W., 1998. Formation of nitroaromatic compounds in advanced oxidation processes: photolysis versus photocatalysis. Environ. Sci. Technol. 33 (2), 294—300.

Echavia, G.R.M., Matzusawa, F., Negishi, N., 2009. Photocatalytic degradation of organophosphate and phosphonoglycine pesticides using TiO_2 immobilized on silica gel. Chemosphere 76 (5), 595—600.

Edzwald, J.K., Becker, W.C., Wattier, K.L., 1985. Surrogate parameters for monitoring organic matter and THM precursors. J. Am. Water Works Assoc. 77 (4), 122—132.

Enriquez, R., Pichat, P., 2001. Interactions of humic acid, quinoline, and TiO_2 in water in relation to quinoline photocatalytic removal. Langmuir 17 (20), 6132—6137.

Fent, K., Weston, A.A., Caminada, D., 2006. Ecotoxicology of human pharmaceuticals. Aquat. Toxicol. 76 (2), 122—159.

Guillard, C., Puzenat, E., Lachheb, H., Houas, A., Herrmann, J.M., 2005. Why inorganic salts decrease the TiO(2) photocatalytic efficiency. Int. J. Photoenergy 7 (1), 1—9.

Haag, W.R., Hoigne, J., 1986. Singlet oxygen in surface waters. 3. Photochemical formation and steady-state concentrations in various types of waters. Environ. Sci. Technol. 20 (4), 341—348.

Herrmann, J.M., 1999. Heterogeneous photocatalysis: fundamentals and applications to the removal of various types of aqueous pollutants. Catal. Today 53 (1), 115—129.

Hoigné, J., Bader, H., 1983. Rate constants of reactions of ozone with organic and inorganic compounds in water—I: non-dissociating organic compounds. Water Res. 17 (2), 173—183.

Huang, W.-J., Chen, L.-Y., Peng, H.-S., 2004. Effect of NOM characteristics on brominated organics formation by ozonation. Environ. Int. 29 (8), 1049—1055.

Huling, S.G., Arnold, R.G., Sierka, R.A., Miller, M.R., 1998. Measurement of hydroxyl radical activity in a soil slurry using the spin trap α-(4-Pyridyl-1-oxide)-N-tert-butylnitrone. Environ. Sci. Technol. 32 (21), 3436—3441.

Hyung, H., Fortner, J.D., Hughes, J.B., Kim, J.-H., 2006. Natural organic matter stabilizes carbon nanotubes in the aqueous phase. Environ. Sci. Technol. 41 (1), 179—184.

Kerc, A., Bekbolet, M., Saatci, A.M., 2003. Sequential oxidation of humic acids by ozonation and photocatalysis. Ozone Sci. Eng. J. Int. Ozone Assoc. 25 (6), 497—504.

Kim, H., Kim, W., Mackeyev, Y., Lee, G.-S., Kim, H.-J., Tachikawa, T., Hong, S., Lee, S., Kim, J., Wilson, L.J., Majima, T., Alvarez, P.J.J., Choi, W., Lee, J., 2012. Selective oxidative degradation of organic pollutants by singlet oxygen-mediated photosensitization: tin porphyrin versus C60 aminofullerene systems. Environ. Sci. Technol. 46 (17), 9606—9613.

Kim, S.D., Cho, J., Kim, I.S., Vanderford, B.J., Snyder, S.A., 2007. Occurrence and removal of pharmaceuticals and endocrine disruptors in South Korean surface, drinking, and waste waters. Water Res. 41 (5), 1013—1021.

Klamerth, N., Malato, S., Agüera, A., Fernández-Alba, A., Mailhot, G., 2012. Treatment of municipal wastewater treatment plant effluents with modified Photo-Fenton as a tertiary treatment for the degradation of micro pollutants and disinfection. Environ. Sci. Technol. 46 (5), 2885—2892.

Klavarioti, M., Mantzavinos, D., Kassinos, D., 2009. Removal of residual pharmaceuticals from aqueous systems by advanced oxidation processes. Environ. Int. 35 (2), 402—417.

Kormann, C., Bahnemann, D.W., Hoffmann, M.R., 1991. Photolysis of chloroform and other organic molecules in aqueous titanium dioxide suspensions. Environ. Sci. Technol. 25 (3), 494—500.

Korshin, G.V., Li, C.-W., Benjamin, M.M., 1997. Monitoring the properties of natural organic matter through UV spectroscopy: a consistent theory. Water Res. 31 (7), 1787—1795.

Kubista, M., Sjoback, R., Eriksson, S., Albinsson, B., 1994. Experimental correction for the inner-filter effect in fluorescence spectra. Analyst 119 (3), 417—419.

Lee, J., Hong, S., Mackeyev, Y., Lee, C., Chung, E., Wilson, L.J., Kim, J.-H., Alvarez, P.J.J., 2011. Photosensitized oxidation of emerging organic pollutants by tetrakis C60 aminofullerene-derivatized silica under visible light irradiation. Environ. Sci. Technol. 45 (24), 10598—10604.

Lee, J., Mackeyev, Y., Cho, M., Li, D., Kim, J.-H., Wilson, L.J., Alvarez, P.J.J., 2009. Photochemical and antimicrobial properties of novel C60 derivatives in aqueous systems. Environ. Sci. Technol. 43 (17), 6604—6610.

Lee, J., Mackeyev, Y., Cho, M., Wilson, L.J., Kim, J.-H., Alvarez, P.J.J., 2010. C60 aminofullerene immobilized on silica as a visible-light-activated photocatalyst. Environ. Sci. Technol. 44 (24), 9488—9495.

Lee, Y., von Gunten, U., 2010. Oxidative transformation of micropollutants during municipal wastewater treatment: comparison of kinetic aspects of selective (chlorine, chlorine dioxide, ferrateVI, and ozone) and non-selective oxidants (hydroxyl radical). Water Res. 44 (2), 555—566.

Li, Q., Mahendra, S., Lyon, D.Y., Brunet, L., Liga, M.V., Li, D., Alvarez, P.J., 2008. Antimicrobial nanomaterials for water disinfection and microbial control: potential applications and implications. Water Res. 42 (18), 4591—4602.

Liao, Y., Brame, J., Que, W., Xiu, Z., Xie, H., Li, Q., Fabian, M., Alvarez, P.J., 2013. Photocatalytic generation of multiple ROS types using low-temperature crystallized anodic TiO2 nanotube arrays. J. Hazard. Mater. 260 (0), 434—441.

Ma, H., Allen, H.E., Yin, Y., 2001. Characterization of isolated fractions of dissolved organic matter from natural waters and a wastewater effluent. Water Res. 35 (4), 985—996.

Maximov, O.B., Glebko, L.I., 1974. Quinoid groups in humic acids. Geoderma 11 (1), 17—28.

Minero, C., Mariella, G., Maurino, V., Vione, D., Pelizzetti, E., 2000. Photocatalytic transformation of organic compounds in the presence of inorganic ions. 2. competitive reactions of phenol and alcohols on a titanium dioxide—fluoride system. Langmuir 16 (23), 8964—8972.

Minero, C., Pelizzetti, E., Sega, M., Friberg, S.E., Sjöblom, J., 1999. The role of humic substances in the photocatlytic degradation of water contaminants. J. Disper. Sci. Technol. 20 (1—2), 643—661.

Paul, A., Stösser, R., Zehl, A., Zwirnmann, E., Vogt, R.D., Steinberg, C.E.W., 2006. Nature and abundance of organic radicals in natural organic matter: effect of pH and irradiation. Environ. Sci. Technol. 40 (19), 5897—5903.

Pereira, J.H.O.S., Reis, A.C., Queirós, D., Nunes, O.C., Borges, M.T., Vilar, V.J.P., Boaventura, R.A.R., 2013. Insights into solar TiO2-assisted photocatalytic oxidation of two antibiotics employed in aquatic animal production, oxolinic acid and oxytetracycline. Sci. Total Environ. 463—464 (0), 274—283.

Qu, X., Brame, J., Li, Q., Alvarez, P.J.J., 2012. Nanotechnology for a safe and sustainable water supply: enabling integrated water treatment and reuse. Acc. Chem. Res. 46 (3), 834—843.

Schindelin, A.J., Frimmel, F.H., 2000. Nitrate and natural organic matter in aqueous solutions irradiated by simulated sunlight — influence on the degradation of the pesticides dichlorprop and terbutylazine. Environ. Sci. Pollut. Res. 7 (4), 205—210.

Schmelling, D.C., Gray, K.A., Kamat, P.V., 1997. The influence of solution matrix on the photocatalytic degradation of TNT in TiO2 slurries. Water Res. 31 (6), 1439—1447.

Schnitzer, M., Khan, S.U., 1972. Humic Substances in the Environment. Marcel Dekker Inc., New York.

Schnitzer, M., Vendette, E., 1975. Chemistry of humic substances extracted from an arctic soil. Can. J. Soil. Sci. 55 (2), 93—103.

Snyder, E.M., Pleus, R.C., Snyder, S.A., 2005. Pharmaceuticals and EDCs in the US water industry — an update. J. Am. Water Works Assoc. 97 (11), 32—36.

Sorensen, M., Tanner, U., Sagawe, G., Frimmel, F.H., 1996. Photochemical degradation of hydrophilic xenobiotics in the UV/H2O2-process. Influence of humic matter on the degradation rate of 2-amino-1-naphthalenesulfonate and ethylenediaminetetraacetate. Acta Hydrochim. Hydrobiol. 24 (3), 132—136.

Steinberg, C.E.W., Kamara, S., Prokhotskaya, V.Y., ManusadŽIanas, L., Karasyova, T.A., Timofeyev, M.A., Jie, Z., Paul, A., Meinelt, T., Farjalla, V.F., Matsuo, A.Y.O., Kent Burnison, B., Menzel, R., 2006. Dissolved humic substances — ecological driving forces from the individual to the ecosystem level? Freshw. Biol. 51 (7), 1189—1210.

Tachikawa, T., Majima, T., 2009. Single-molecule fluorescence imaging of TiO$_2$ photocatalytic reactions. Langmuir 25 (14), 7791—7802.

Ternes, T.A., Stuber, J., Herrmann, N., McDowell, D., Ried, A., Kampmann, M., Teiser, B., 2003. Ozonation: a tool for removal of pharmaceuticals, contrast media and musk fragrances from wastewater? Water Res. 37 (8), 1976—1982.

Thurman, E.M., 1985. Organic Geochemistry of Natural Waters. Springer Netherlands, Boston, MA.

Toor, R., Mohseni, M., 2007. UV-H2O2 based AOP and its integration with biological activated carbon treatment for DBP reduction in drinking water. Chemosphere 66 (11), 2087—2095.

Topudurti, K., Wojciechowski, M., Anagnostopoulos, S., Eilers, R., 1998. Field evaluation of a photocatalytic oxidation technology. Water Sci. Technol. 38 (7), 117—125.

Wilkinson, F., Helman, W.P., Ross, A.B., 1995. Rate constants for the decay and reactions of the lowest electronically excited singlet state of molecular oxygen in solution. An expanded and revised compilation. J. Phys. Chem. Ref. Data 24 (2), 663—677.